Holographic QCD methods for quarkonium production

Kiminad Mamo (William & Mary)

April 16, 2025 @ Exotic heavy meson spectroscopy and structure at the EIC, CFNS, Stony Brook

References

This talk is based on:

- **1910.04707** (PRD) (with Ismail Zahed)
- **2106.00722** (PRD) (with Ismail Zahed)
- **2204.08857** (PRD) (with Ismail Zahed)
- **2109.03103** (PRD) (with Yizhuang Liu, Maciej A. Nowak, Ismail Zahed)
- **2401.12162** (PRD) (with Florian Hechenberger, Ismail Zahed)

AdS/CFT

- The AdS/CFT correspondence can be used to compute correlation functions of local operators [Maldacena (1998); Gubser, Klebanov, Polyakov (1998); Witten (1998)]:

$$Z_{\text{gauge}}(J\mathcal{O}, N_c, \lambda) \equiv Z_{\text{gravity}}(\phi_0, g_5, \alpha'/R^2), \quad \text{where } J \equiv \phi_0.$$

- Correlation functions are evaluated via Witten diagrams in AdS.
- For non-conformal theories with a mass gap (dual to a deformed AdS background), scattering amplitudes can likewise be computed using these Witten diagrams in AdS

$$ds^2 = \frac{R^2}{z^2}\left(\eta_{\mu\nu}\, dx^\mu dx^\nu - dz^2\right), \quad \eta_{\mu\nu} = \mathrm{diag}(1, -1, -1, -1),$$

with $0 \le z \le \infty$, connects the UV boundary ($z \to 0$) to the IR ($z \to \infty$), and mass gap/confinement induced by a background dilaton field $\phi(z) = \kappa^2 z^2$.

Two-point function

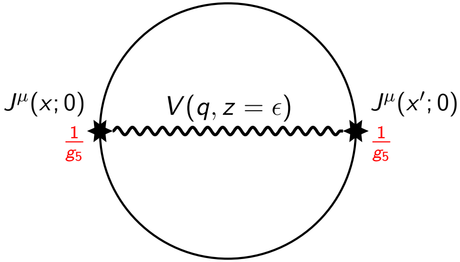

Figure: Witten diagram for the two-point function of the current operator with $g_5^2 \sim \frac{1}{N_c}$.

- The bulk-to-boundary propagator for the virtual photon is

$$\mathcal{V}(Q,z) = g_5 \sum_n \frac{F_n\,\phi_n(z)}{Q^2+m_n^2} = \Gamma\left(1+\frac{Q^2}{4\kappa^2}\right)\kappa^2 z^2\, \mathcal{U}\left(1+\frac{Q^2}{4\kappa^2}; 2; \kappa^2 z^2\right),$$

where Γ is the Gamma function and $\mathcal{U}$ is the Tricomi confluent hypergeometric function.

Spin-1 (Electromagnetic) Form Factors of Proton

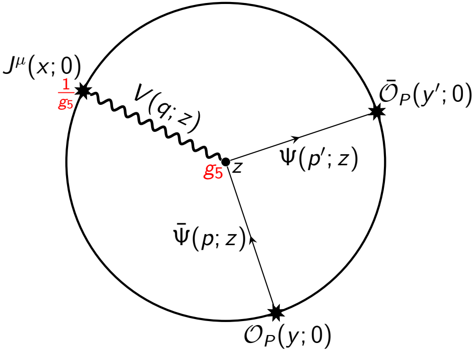

Figure: Witten diagram for EM form factor due to the exchange of vector mesons with $g_5^2 \sim \frac{1}{N_c}$.

Spin-1 (Electromagnetic) Form Factors of Proton

- The scattering amplitude in AdS is

$$S^{EM}_{Dirac}[i,f] = (2\pi)^4\,\delta^4(p'-p-q)\,\frac{1}{g_5}\times g_5\,\overline{u}_{s_f}(p')\,\epsilon_\mu(q)\gamma^\mu\,u_{s_i}(p)$$

$$\times\frac{1}{2}\int\frac{dz}{z^{2M}}\,e^{-\phi}\,\mathcal{V}(Q,z)\left(\psi_L^2(z)+\psi_R^2(z)\right).$$

Spin-2/0 (Gravitational) Form Factors of Proton

- The gravitational form factors (GFFs) of the proton are defined via the energy-momentum tensor (EMT):

$$\langle p_2 \mid T^{\mu\nu}(0) \mid p_1 \rangle = \overline{u}(p_2)\left(A(k)\gamma^{(\mu}p^{\nu)} + B(k)\,\frac{i\,p^{(\mu}\sigma^{\nu)\alpha}k_\alpha}{2m_N} + C(k)\,\frac{k^\mu k^\nu - \eta^{\mu\nu}k^2}{m_N} \right) u(p_1),$$

with $k = p_2 - p_1$. Often one writes $D(k) \equiv 4\,C(k)$.

- The bulk metric fluctuations decompose into spin-2 (transvers-traceless part h) and spin-0 (traceful part f) [Kanitscheider (2008)]:

$$h_{\mu\nu}(k,z) \supset \left[\epsilon^{TT}_{\mu\nu}\, h(k,z)\right] + \left[\tfrac{1}{3}\,\eta_{\mu\nu}\, f(k,z)\right].$$

- For non-degenerate 2^{++} and 0^{++} glueball spectra, the holographic coupling includes both transverse-traceless (spin-2) and scalar (spin-0) fluctuations, respectively.

Spin-2/0 (Gravitational) Form Factors of Proton

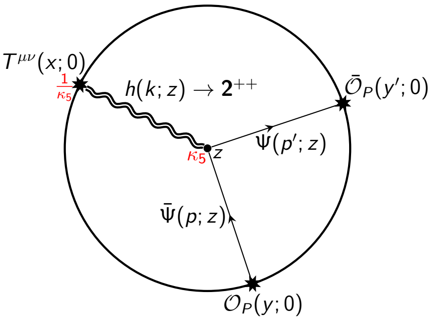

Figure: Witten diagram for spin-2 gravitational form factor due to the exchange 2^{++} glueballs with $\kappa_5^2 \sim \frac{1}{N_c^2}$.

$$A(K,\kappa_T) \;=\; \frac{1}{2}\int dz\,\sqrt{g}\,e^{-\phi}\,z\,\left(\psi_R^2(z)+\psi_L^2(z)\right)\sum_{n=0}^{\infty}\frac{\sqrt{2}\,\kappa_5\,F_n\,\psi_n(z)}{K^2+m_n^2}.$$

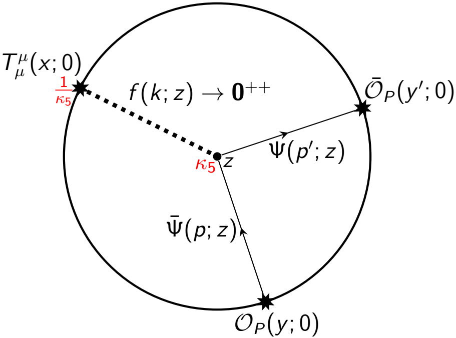

Figure: Witten diagram for scalar gravitational form factor due to the exchange 0^{++} glueballs.

$$D(K,\kappa_T,\kappa_S) = -\frac{4\,m_N^2}{3\,K^2}\Big[A(K,\kappa_T)\;-\;A_S(K,\kappa_S)\Big],$$

Comparison with Lattice Data

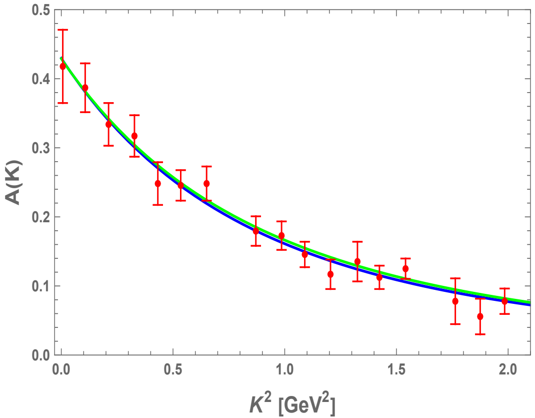

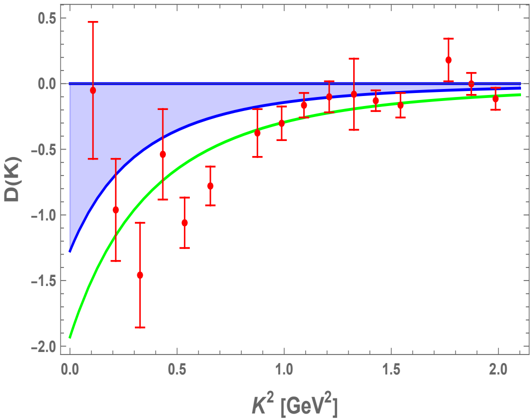

Recent lattice QCD results [Pefkou:2021] (red points) compared to holographic fits (blue curves) with $\kappa_T = 0.388\,\mathrm{GeV}$, $\kappa_S = 0.217\,\mathrm{GeV}$. The green line is a tripole fit to the same lattice data.

Photoproduction of Heavy Mesons Near Threshold

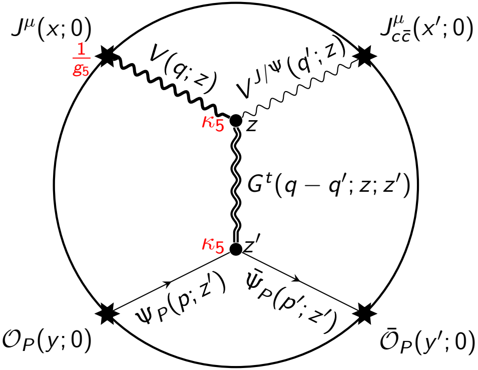

Figure: Witten diagrams for the holographic photo/electroproduction of J/Ψ with $g_5^2 \sim \frac{1}{N_c}$ and $\kappa_5^2 \sim \frac{1}{N_c^2}$.

Photoproduction of heavy mesons near threshold

- the differential cross section for photoproduction of heavy vector mesons (J/ψ or Υ), near threshold, is given by

$$\begin{aligned}\frac{d\sigma}{dt} &= \mathcal{N}^2 \times \left[A(t) + \eta^2 D(t)\right]^2 \\ &\times \frac{1}{A^2(0)} \times \frac{1}{32\pi(s - m_N^2)^2} \times F(s, t, M_V, m_N) \times \left(1 - \frac{t}{4m_N^2}\right)\end{aligned}$$

with the normalization factor $\mathcal{N}$ defined as

$$\mathcal{N}^2 \equiv e^2 \times \left(\frac{f_V}{M_V}\right)^2 \times \mathbb{V}^2_{h\gamma^* J/\Psi} \times (2\kappa_5^2)^2 \times A^2(0) = 7.768^2\, \mathrm{nb}/\mathrm{GeV}^6$$

- note that $F(s, t) \sim s^4 \sim 1/\eta^4$ with the amplitude $\mathcal{A} \sim s^2 \times A(t) + s^0 \times D(t)$ as expected from 2^{++} and 0^{++} glueball t-channel exchanges

Extraction of the 2^{++} glueball contribution

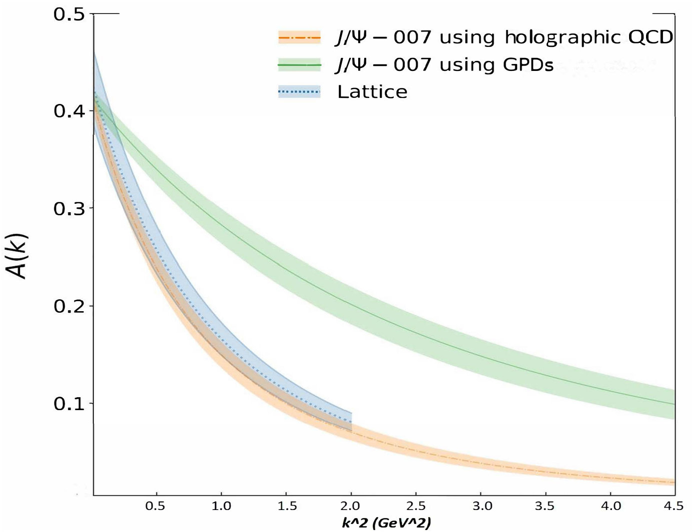

Extraction of the 0^{++} glueball contribution

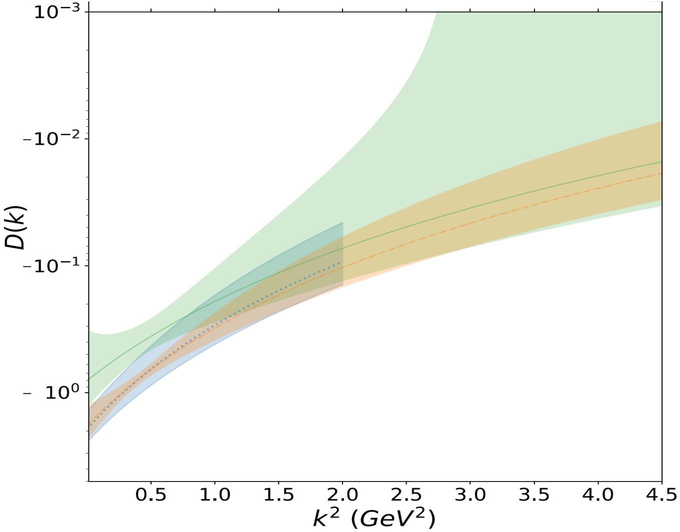

Electroproduction of heavy mesons near threshold

- the differential cross section for electroproduction of heavy vector mesons (J/ψ or Υ), near threshold, is given by

$$\frac{d\sigma(s,t,Q,M_{J/\Psi},\epsilon_T,\epsilon'_T)}{dt} \propto \mathcal{I}^2(Q,M_{J/\Psi}) \times \left(\frac{s}{\kappa^2}\right)^2 \times \left[A(t)+\eta^2 D(t)\right]^2$$

$$\frac{d\sigma(s,t,Q,M_{J/\Psi},\epsilon_L,\epsilon'_L)}{dt} \propto \frac{1}{9} \times \frac{Q^2}{M^2_{J/\Psi}} \times \mathcal{I}^2(Q,M_{J/\Psi}) \times \left(\frac{s}{\kappa^2}\right)^2 \times \left[A(t)+\eta^2 D(t)\right]^2$$

Electroproduction of heavy mesons near threshold

- where we defined the transition form factor that controls the Q dependence as

$$\mathcal{I}(Q, M_{J/\Psi}) = \frac{\mathcal{I}(0, M_{J/\Psi})}{\frac{1}{6}\times\left(\frac{Q^2}{4\kappa_{J/\Psi}^2}+3\right)\left(\frac{Q^2}{4\kappa_{J/\Psi}^2}+2\right)\left(\frac{Q^2}{4\kappa_{J/\Psi}^2}+1\right)},$$

with $\mathcal{I}(0, M_{J/\Psi}) = \frac{g_5 f_{J/\Psi}}{4M_{J/\Psi}}$

Electroproduction of heavy mesons near threshold

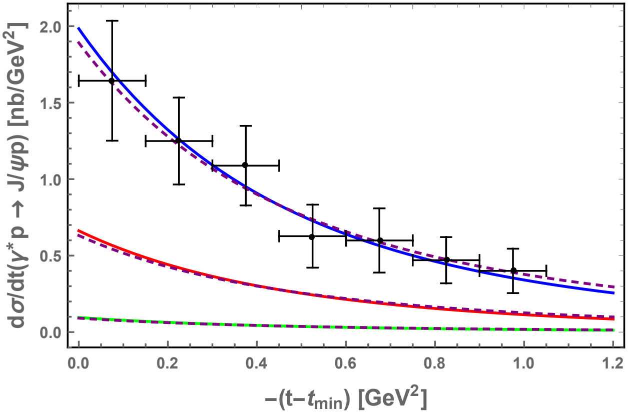

Figure: The variation of the total differential cross section with t and Q^2 for $s = 21\ GeV^2$. The blue curve is for $Q = 0$. The red curve is for $Q = 1.2\ GeV$. The green curve is for $Q = 2.2\ GeV$. The data is from GlueX collaboration at JLab in 2019.

Electroproduction of heavy mesons near threshold

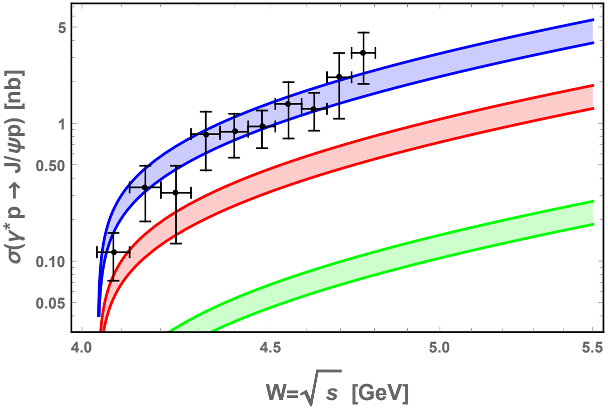

Figure: The variation of the total cross section (near threshold) with Q^2 and $\sqrt{s}$. The blue band is for $Q^2 = 0$ (the data is from GlueX in 2019), the red band is for $Q^2 = 1.2^2$ GeV^2, the green band is for $Q^2 = 2.2^2$ GeV^2.

Electroproduction of heavy mesons near threshold

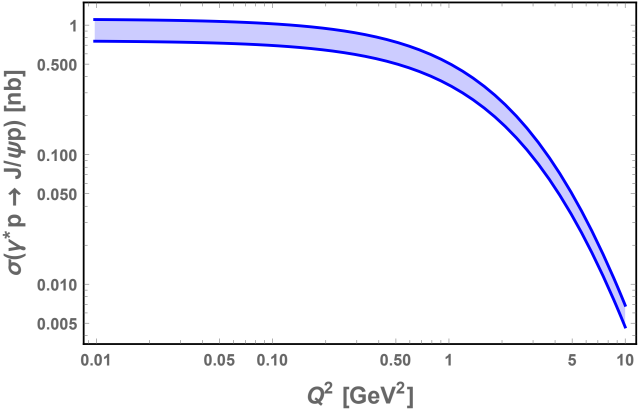

Figure: The variation of the total cross section with Q^2 (near threshold), s=W$^2 = 4.4^2$ GeV^2.

Electroproduction of heavy mesons near threshold

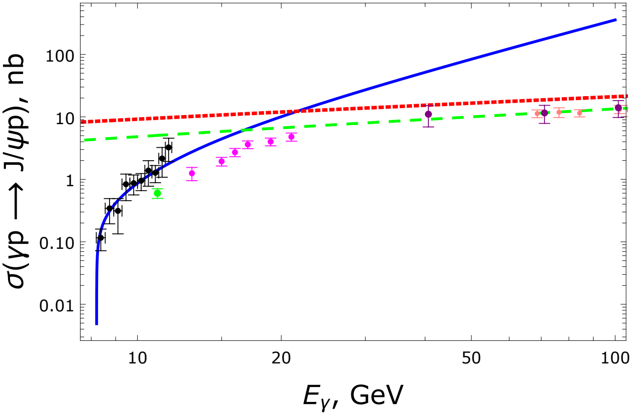

Figure: The total cross section for J/Ψ photoproduction.

Pentaquarks at JLab and EIC

- The masses and total widths of the three charm pentaquark states reported by LHCb [Aaij:2019] are

$$
\begin{aligned}
m_{P_c} &= 4311.9 \pm 0.7\,\mathrm{MeV} \qquad \Gamma_{P_c} = 9.8 \pm 2.7\,\mathrm{MeV} \\
m_{P_c} &= 4440.3 \pm 1.3\,\mathrm{MeV} \qquad \Gamma_{P_c} = 20.6 \pm 4.9\,\mathrm{MeV} \\
m_{P_c} &= 4457.3 \pm 0.6\,\mathrm{MeV} \qquad \Gamma_{P_c} = 6.4 \pm 2.0\,\mathrm{MeV}
\end{aligned}
$$

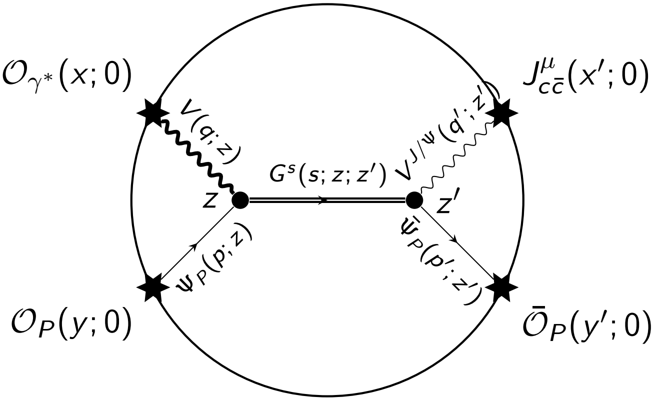

(a)

Figure: Witten diagram for the holographic **s-channel** electroproduction of J/Ψ.

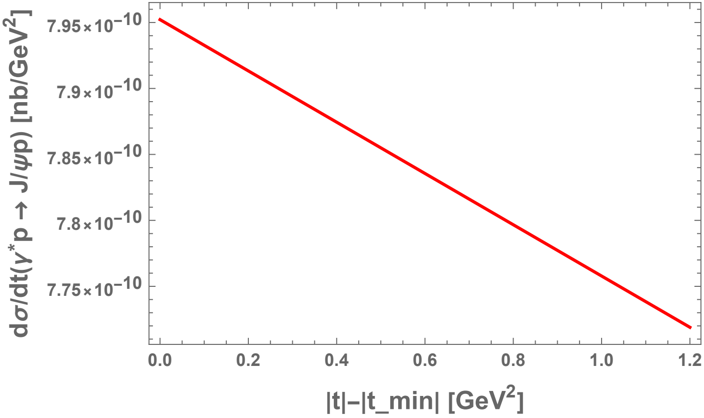

Figure: s-channel contribution to the photo-production differential cross section for $V = J/\Psi$, including all three charm pentaquark contributions.

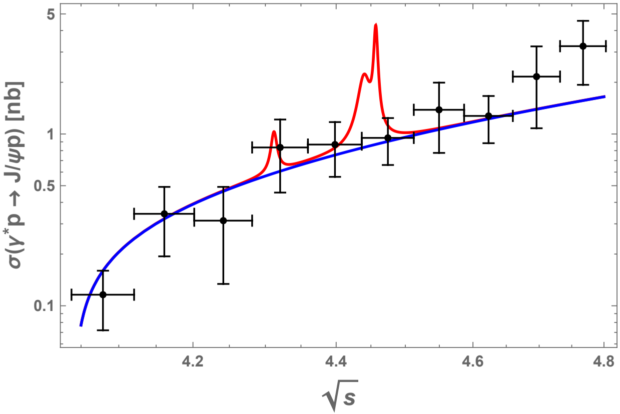

Figure: Total cross section for $V = J/\Psi$ photo-production: the blue-solid curve is our t-channel contribution, the red-solid curve is the sum of t- and s-channel contribution showing the three holographic pentaquarks times $\mathcal{N}_s = 2.0 \times 10^6$ to make them visible, and the data is from [GlueX:2019].

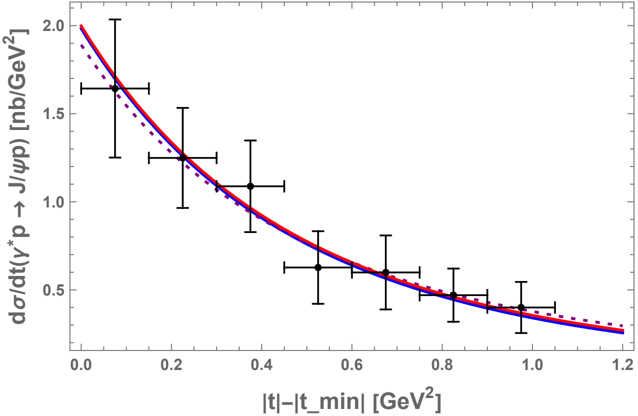

Figure: s-channel plus t-channel contributions to the photo-production differential cross section for $V = J/\Psi$, including all three charm pentaquark contributions. The blue-solid and dashed-purple curves are the holographic t-channel contributions. The solid-red line is the total s- and t-channel contribution with the s-channel contribution multiplied by $\mathcal{N}_s = 2.0 \times 10^7$ to make it slightly visible. The data are from [GlueX:2019] at $\sqrt{s} = 4.6\,\mathrm{GeV}$.

Holographic search for exotics at JLab and EIC

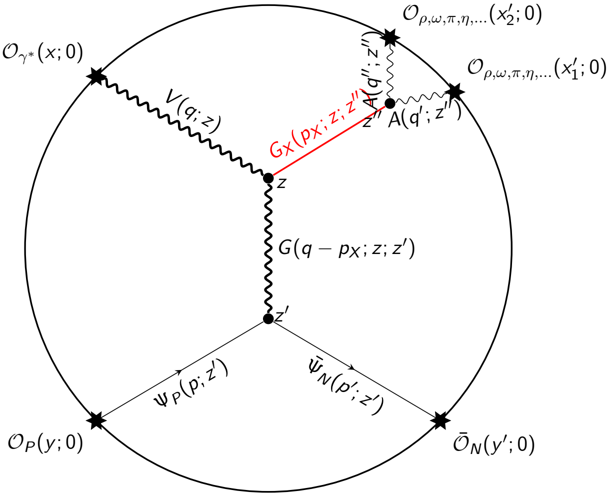

Figure: A general t-channel Witten diagram for exotics at JLab and EIC.

$$V_\mu = V_\mu^a T^a + \frac{\tilde{V}_\mu}{\sqrt{4}} \mathbf{1}_{4\times 4}$$

$$V_\mu = \begin{pmatrix} \frac{\rho_\mu^0}{\sqrt{2}} + \frac{\omega_\mu}{\sqrt{6}} + \frac{\phi_\mu}{\sqrt{12}} & \rho_\mu^+ & K_\mu^{*+} & D_\mu^{*0} \\ \rho_\mu^- & -\frac{\rho_\mu^0}{\sqrt{2}} + \frac{\omega_\mu}{\sqrt{6}} + \frac{\phi_\mu}{\sqrt{12}} & K_\mu^{*0} & D_\mu^{*+} \\ K_\mu^{*-} & \bar{K}_\mu^{*0} & -\frac{2\omega_\mu}{\sqrt{6}} + \frac{\phi_\mu}{\sqrt{12}} & D_\mu^{*-} \\ \bar{D}_\mu^{*0} & D_\mu^{*-} & \bar{D}_\mu^{*0} & -\frac{3\phi_\mu}{\sqrt{12}} \end{pmatrix} + \frac{\tilde{V}_\mu}{\sqrt{4}} \mathbf{1}_{4\times 4}$$

and

$$B = B^a T^a + \frac{\tilde{B}}{\sqrt{4}} \mathbf{1}_{4\times 4}$$

$$B = \begin{pmatrix} \frac{\Sigma^0}{\sqrt{2}} + \frac{\Lambda}{\sqrt{6}} + \frac{B^0}{\sqrt{12}} & \Sigma^+ & p & \Sigma_c^{++} \\ \Sigma^- & -\frac{\Sigma^0}{\sqrt{2}} + \frac{\Lambda}{\sqrt{6}} + \frac{B^0}{\sqrt{12}} & n & \Sigma_c^+ \\ \Xi^- & \Xi^0 & -\frac{2\Lambda}{\sqrt{6}} + \frac{B^0}{\sqrt{12}} & \Xi_c^0 \\ \Xi_c^- & \Xi_c^0 & \Omega_c & -\frac{3B^0}{\sqrt{12}} \end{pmatrix} + \frac{\tilde{B}}{\sqrt{4}} \mathbf{1}_{4\times 4}$$

$$\mathcal{L}_{\text{int}} = \frac{1}{2}\, g_5\, f^{abc} \left(\partial_\mu V_\nu^a - \partial_\nu V_\mu^a\right) V^{\mu\, b} V^{\nu\, c} - \frac{1}{4}\, g_5^2\, f^{abc} f^{ade}\, V_\mu^b V_\nu^c\, V^{\mu\, d} V^{\nu\, e}\,.$$

$$\mathcal{L}_{\text{CS}} \subset g_5 \epsilon^{MNPQR}\, \mathrm{Tr}\left[A_M \tilde{F}_{NP}(V) \tilde{F}_{QR}(V) + A_M \tilde{F}_{NP}(A) \tilde{F}_{QR}(A)\right].$$

$$\mathcal{L}_{\text{int}} = -i \frac{g}{2} f^{abc} V_\mu^a \bar{B}^c \gamma^\mu B^b$$

Summary

- **AdS/CFT Approach:** Witten diagrams in a confining AdS background capture QCD correlators and scattering amplitudes.
- **Form Factors:** Proton gravitational form factors arise from metric fluctuations (corresponding to 2^{++}, and 0^{++} glueballs), matching lattice and experimental data.
- **Near-Threshold Production:** Holographic amplitudes for photoproduction of heavy quarkonia (J/ψ, Υ)
- **Electroproduction & Q^2:** Virtual photon effects enter through a transition form factor with multi-pole behavior, describing electroproduction cross sections at various kinematics.
- **Pentaquarks (s-channel):** Possible s-channel resonances (pentaquarks) appear near threshold in addition to dominant t-channel glueball exchanges, offering predictions for JLab and EIC.

Thank You!